Available online at www.sciencedirect.com

SciVerse ScienceDirect

Ceramics International 38 (2012) 6405–6410

CERAMICS INTERNATIONAL

www.elsevier.com/locate/ceramint

Characterization of $La_{0.67}Sr_{0.33}MnO_z$ thin films synthesized by metal-organic decomposition on different substrates

Xiangrong Zhu[a,b,*], Honglie Shen[c], Koichi Tsukamoto[d], Takeshi Yanagisawa[d], Mamoru Okutomi[d], Noboru Higuchi[d]

[a]*School of Urban Development and Environmental Engineering, Shanghai Second Polytechnic University, 2360 Jinhai Road, Shanghai 201209, PR China*
[b]*State Key Laboratory of Functional Materials for Informatics, Shanghai Institute of Microsystem and Information Technology, Chinese Academy of Sciences, 865 Changning Road, Shanghai 200050, PR China*
[c]*College of Materials Science & Technology, Nanjing University of Aeronautics & Astronautics, Nanjing 211100, PR China*
[d]*National Institute of Advanced Industrial Science and Technology, 1-1-4 Umezono, Tsukuba, Ibaraki 305-8568, Japan*

Received 1 April 2012; received in revised form 18 April 2012; accepted 4 May 2012
Available online 17 May 2012

Abstract

$La_{0.67}Sr_{0.33}MnO_z$ (LSMO) thin films were synthesized by means of metal-organic decomposition on the substrates including amorphous quartz, (1 0 0) Si chip, (1 0 0) MgO single crystal and polycrystalline Al_2O_3 ceramic plate. The structure and magnetotransport properties of the films were characterized. X-ray diffraction spectra show that all samples are polycrystalline with (2 0 2) preferred orientation. All films present metal–insulator transition and enhanced magnetoresistance (MR) effect below metal–insulator transition peak temperature (T_p). At room temperature (RT) low-field magnetoresistance effect (LFMR) and linear change of resistivity under applied field are exhibited by all the films. These magnetotransport properties were first ascribed to the porous structural characteristics in the films observed by atomic force microscope. Furthermore, the LSMO film synthesized on (1 0 0) MgO substrate presents a bit different magnetic properties and magnetotransport from the other samples, including broad ferromagnetic–paramagnetic transition zone, lower T_p and weaker LFMR at RT. However, for the samples synthesized on the other substrates, the LFMR effect is very similar to each other and their MR ratio reaches near 5% under 10 kOe field. Thus the substrate effect of LSMO film on (1 0 0) MgO is more intensive than that of the other samples.

Keywords: A. Metal-organic decomposition; B. Structure; C. Magnetotransport; D. LSMO film

1. Introduction

$La_{0.67}Sr_{0.33}MnO_3$ (LSMO), as one kind of perovskite manganites, has been intensively researched for two decades because of its colossal magnetoresistance (CMR) properties [1–3], large magnetocaloric effect [4] and perfect temperature dependence of resistance (TCR) [5]. Especially, LSMO presents high spin polarization and then becomes one research focus of so-called spintronics [6]. Considering the application requirement on devices such as highly sensitive magnetic sensors, magnetic random access memory, etc., the research on LSMO films is vital. Usually, LSMO films are epitaxial or polycrystalline. On the one hand, most of epitaxial LSMO films are synthesized on single crystalline substrates such as (1 0 0) $LaAlO_3$ or (1 0 0) $SrTiO_3$ whose lattice constants are close to that of LSMO [7,8]. High CMR ratio is shown by the epitaxial LSMO films. On the other hand, compared to epitaxial LSMO films, the polycrystalline LSMO films with some certain structural defects such as grain boundaries or oxygen-deficient would bring forth the so-called large low-field MR (LFMR) effect [9–11]. Namely, MR ratio would change steeply over low field range below Curie temperature (T_C), which is significant for the application of LSMO films. The spin-polarized intergrain tunneling and the spin-dependent

*Corresponding author at: School of Urban Development and Environmental Engineering, Shanghai Second Polytechnic University, 2360 Jinhai Road, Shanghai 201209, PR China. Tel.: +86 21 50215021x8536; fax: +86 21 50217725.
E-mail address: zhuxiangrong71@126.com (X. Zhu).

0272-8842/$36.00
http://dx.doi.org/10.1016/j.ceramint.2012.05.013

scattering at interfaces or grain boundaries are ascribed to LFMR effect [9–11]. Thus structural defects play very important roles in the magnetotransport of polycrystalline LSMO.

LSMO thin films have been mainly prepared by pulsed laser deposition (PLD) [12], magnetron sputtering [13], molecular beam epitaxy [14] and metal-organic chemical vapor deposition (MOCVD) [15]. All these methods require large, complex and expensive equipment. In contrast, solution deposition methods for oxide films such as sol–gel and metal-organic decomposition (MOD) as convenient and economical techniques have been used to synthesize LSMO films [16,17]. Moreover for the sake of controlling the application cost, the use of cheap substrates such as amorphous quartz, ceramics and silicon wafer should be considered while synthesizing the LSMO films. At the same time, the effect of substrates on structure and magnetotransport should be investigated.

Once we have reported the MOD growth of $La_{0.67}Sr_{0.33}MnO_z$ films on amorphous quartz substrates under different annealing temperature and compared their structural characteristics and magnetotransport properties [17]. In this article, we would like to further report the MOD synthesis of $La_{0.67}Sr_{0.33}MnO_z$ films on other substrates including (1 0 0) silicon chip, (1 0 0) MgO single crystal and polycrystalline Al_2O_3 ceramics besides on amorphous quartz. The structural characteristics and magnetotransport properties of the samples are characterized and compared in detail.

2. Experimental

Before MOD process, the four kinds of substrates were made from amorphous quartz, (1 0 0) Si wafer, (1 0 0) MgO single crystal plate and polycrystalline Al_2O_3 ceramic plate. The size of each substrate was 1 cm × 1.5 cm. All substrates were cleaned by ultrasonic cleaner and dried in an oven. For the MOD experiment, the starting solutions, $LaO_{1.5}$, $MnO_{1.5}$ and SrO, were purchased from Symetrix Corporation in Japan. Their molar concentrations were 0.1–0.5 mol/l. According to the nominal composition of $La_{0.67}Sr_{0.33}MnO_z$, the above starting solutions were mixed in such a way that the molar ratio of La:Sr:Mn was consistent with 2:1:3. Here, the oxygen composition is marked as z because the MOD annealing technique was conducted in air, which would result in the minor deviation of oxygen and non-stoichiometric oxygen. The mixed solutions were used as precursor solutions, spin-coated on the above clean substrates to form wet films. Then the wet films were baked in air at 473 K for 10 min. In order to increase the film thickness, the above process of preparing and baking gel films was repeated twice. After the baking, the gel films were annealed in air at 993 K for 50 min. After annealing all the samples were slowly cooled down to room temperature (RT) by shutting off the heat treatment system.

The samples were coded with LSMQ, LSMS, LSMM and LSMC, corresponding to their substrates, amorphous quartz, (1 0 0) Si chip, (1 0 0) MgO single crystal and polycrystalline Al_2O_3 ceramic. Rutherford backscattering spectra showed that the composition of the metallic elements in the films varied from that of the corresponding concocted solutions by about 5% and the thickness of the films was about 1000–1200 Å. For all samples, the crystalline structure was determined by X-ray diffractometer (XRD). The surface morphologies were observed by atomic force microscope (AFM). The magnetotransport properties were measured by means of standard four-probe technique over a temperature range from 77 K to RT while the probe current was parallel to the longitudinal direction of the films and the magnetic field was applied along the current direction. Finally, the temperature dependence of magnetization of LSMQ and LSMM were obtained from SQUID magnetometer.

3. Results and discussion

The XRD spectra of all samples are shown in Fig. 1. First, a very strong peak is exhibited on the XRD spectra of LSMM and LSMS, which should be the diffracting peak of (1 0 0) MgO and (1 0 0) Si substrates. Secondly, several indexed peaks in the XRD spectra of the samples except LSMC reveal the typical polycrystalline perovskite structural characteristics and the (2 0 2) peaks are much higher than the other indexed LSMO peaks, indicating the (2 0 2) preferred orientation of the films. It should be pointed out that, although the LSMM sample presents polycrystalline characteristics, epitaxial LSMO film on (1 0 0) MgO substrate could be still prepared by other techniques such as magnetron sputtering [18] and dipping–pyrolysis process [19]. Thirdly, for LSMC sample, the XRD spectra show multiple peaks, reflecting complex polycrystalline structure of Al_2O_3 ceramic substrate. However, the (2 0 2) peak of LSMO film could be still identified. Finally, the 2θ data of (2 0 2) peaks of all the samples are 32.850°, 32.808°, 32.750° and 32.620°, corresponding to LSMQ, LSMS, LSMM and LSMC, respectively. Since these 2θ data of (2 0 2) peaks are close, it could be deduced that the difference of lattice constants among the samples is slight. Usually for $La_{1-x}Sr_xMnO_3$ materials, the lattice structure is firstly determined by x, the content of Sr [20]. The above XRD results indicate that, for the polycrystalline LSMO samples synthesized by MOD technique, different substrates would slightly change the lattice constants of the LSMO films.

The 5 μm × 5 μm AFM images of the surface morphology of all the polycrystalline LSMO films except LSMC are displayed in Fig. 2. It can be observed that, for each sample, near round particles were grown smoothly and uniformly on the substrate. The size of the particles ranges from 200 nm to 300 nm. At the same time, the structure of each film seems a bit porous, meaning the films are not dense and the grain boundaries are weakly linked. In general the surface morphology characteristics are similar to each other for these samples regardless of the different substrates. Furthermore, the surface root mean square (RMS) roughness is 8.2 nm for LSMQ, 9.3 nm for LSMS and 10.4 nm for LSMM, indicating that LSMM presents

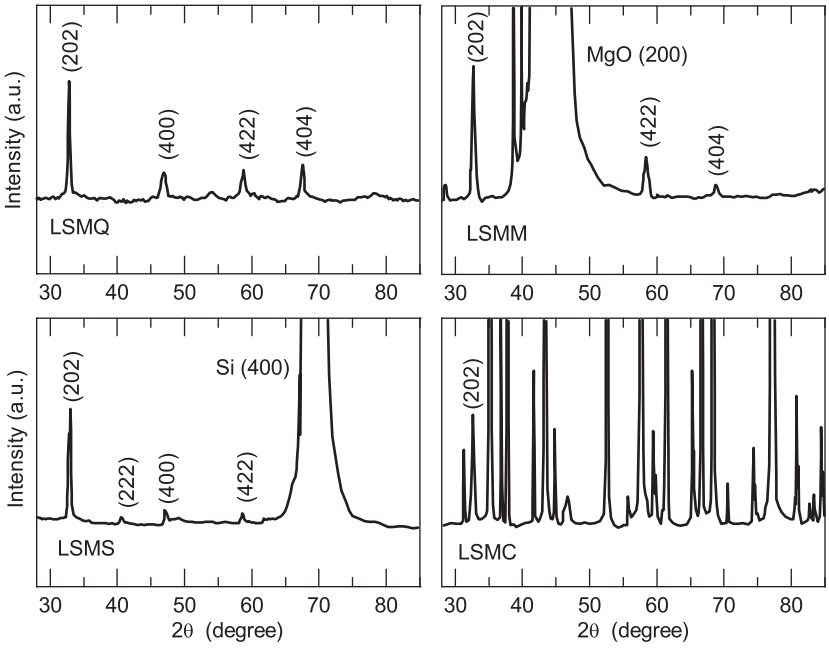

Fig. 1. XRD spectra of all LSMO films on different substrates.

higher RMS and its grain size should be larger. Specially, for LSMC sample, the surface of ceramic substrate is very coarse and AFM operation conducted on the sample is very difficult. The quality of the AFM images is very poor. So the AFM image of LSMC is not shown in Fig. 2. Certainly it could be still believed that there should also exist porous structural characteristics for LSMC sample.

Fig. 3 exhibits the temperature dependences of magnetization under 50 Oe after zero field cooling (ZFC) for LSMQ and LSMM samples. Both of the two samples present typical ferromagnetic–paramagnetic transition. However the ferromagnetic–paramagnetic transition zone for LSMQ is steep and for LSMM is relatively broad. Despite of the obvious difference of ferromagnetic–paramagnetic transition zone, the Curie Temperature (T_C) for the two samples is close. For LSMQ, T_C is 335 K and for LSMM, 330 K, about 30 K lower than that of single crystal $La_{0.67}Sr_{0.33}MnO_3$ [21], which should originate from the oxygen-deficient of the samples [11].

Usually for the magnetic behavior of epitaxial LSMO thin films, especially ultra thin films, the effect of the film stress or strain caused by substrates could not be neglected [22–24]. The ferromagnetism of the film or the pattern of temperature dependence of magnetization would change more or less with the degree of compressive or tensile strain of the film. For the LSMQ and LSMM samples, although they are polycrystalline and the thickness of the LSMO films is beyond 100 nm, the effect of film stress or strain on the magnetic behavior might also be considered. The broad ferromagnetic–paramagnetic transition zone for LSMM indicates that the effect of MgO substrate is more intensive than that of amorphous quartz substrate. Majumdar et al. [24] also observed broad ferromagnetic–paramagnetic transition zone for the 400 nm-thickness LSMO film on (1 0 0) MgO single crystal, which was just ascribed to the film strain.

For all the samples, their temperature dependences of resistivity under zero field and MR ratio under 8 kOe field from 77 K to RT are plotted in Fig. 4. MR ratio is defined as $(\rho_0-\rho_H)/\rho_0\times 100\%$, where ρ_0 is the resistivity under zero field and ρ_H is the resistivity under applied 8 kOe field. First, the resistivity–temperature dependence of each sample under zero field shows only one peak, namely the typical metal–insulator transition peak. The data of metal–insulator transition peak temperature (T_p) are 227 K, 232 K, 187 K and 242 K for LSMQ, LSMS, LSMM and LSMC, respectively. It could be noticed that T_p of LSMQ and LSMM is far lower than T_C obtained from Fig. 3. Furthermore, the T_p data of LSMQ, LSMS and LSMC are close. For LSMM, T_p is lowest, which is lowered from 40 K to 55 K than the other samples. Secondly, the MR ratio of each sample under 8 kOe field monotonously increases with the temperature decreasing from RT to 77 K, and no MR peak appears near T_p, exhibiting a strong enhanced MR effect over the temperature range below T_p. This kind of magnetotransport behavior is unlike that of the single crystal LSMO [20] or epitaxial LSMO film [21], for which the MR would decline steeply when the temperature decreases from T_p. Thirdly, the difference of MR ratio of the samples could be noticed. At 77 K, the MR ratio of LSMM is highest, reaching 17%. For LSMC sample, the MR ratio is lowest, 10%. However, at 297 K (RT) the MR ratio for LSMM is lowest, 2% and for the other three samples is similar, about 4%.

In general, the above results indicate that samples present similar pattern of temperature dependence of magnetotransport. In our previous research [17], the effect of structural characteristics on the magnetotransport of

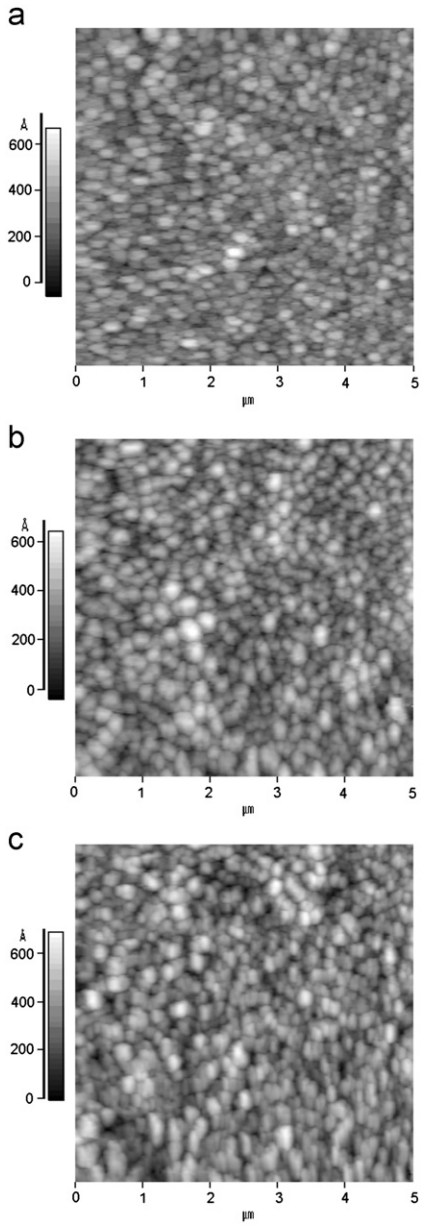

Fig. 2. 5 μm × 5 μm AFM images of surface morphology of LSMQ (a), LSMS (b) and LSMC (c).

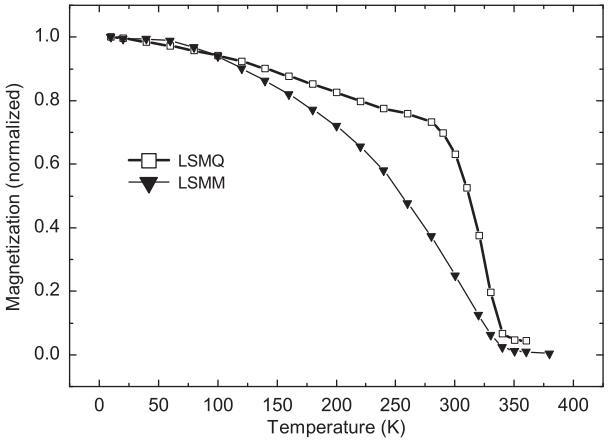

Fig. 3. Temperature dependences of magnetization under 50 Oe field after zero field cooling for LSMQ and LSMM samples.

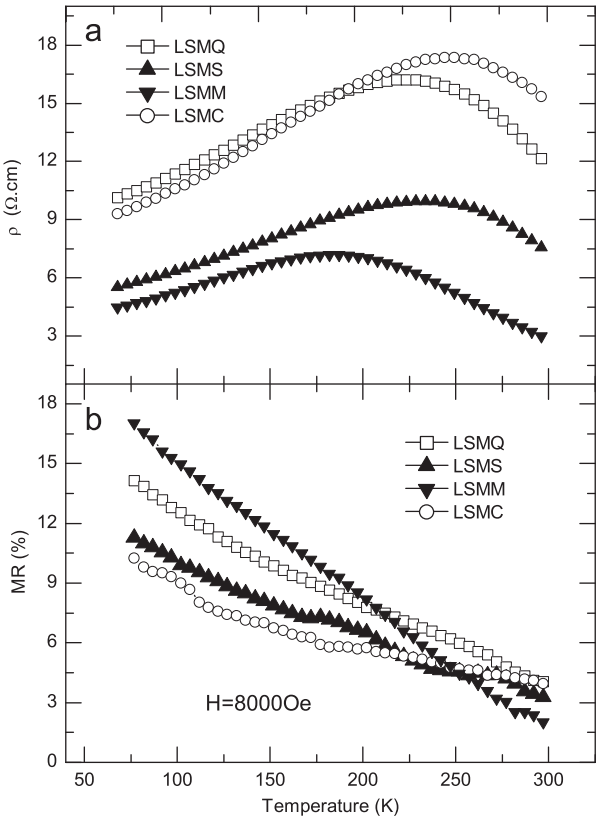

Fig. 4. Temperature dependences of resistivity under zero field and MR ratio under 8 kOe field for all the LSMO films.

LSMO films synthesized on amorphous quartz under different annealing temperature has been discussed. For those samples, AFM images showed that their structure was a bit porous. These structural defects could cause weak-linked grain boundaries, where the alignment of spins becomes easy and thus strong enhanced MR behavior occurs below metal–insulator transition temperature [25]. The defects of porosity were intrinsic structural characteristics of those samples and were not sensitive to the grain size of LSMO film. Thus the magnetotransport behaviors would be dominated by structural defects of porosity. In this paper, the common structural characteristics for the samples is also porous regardless of the different substrates, as discussed above, which should be also responsible for the magnetotransport behaviors shown by Fig. 4. Especially for LSMM sample, the effect of substrate of MgO should be considered additionally, which might be responsible for the lowest T_p. The more similarity of magnetotransport of LSMQ, LSMS and LSMC further reveals the less effect of their substrates.

The field dependences of resistivity of all samples were investigated at RT (about 297 K). As shown in Fig. 5, for each sample, when the applied field H is scanned from +10 kOe to −10 kOe and back, the normalized resistivity ρ_H/ρ_{max} changes linearly over wide field range. Here, ρ_{max}

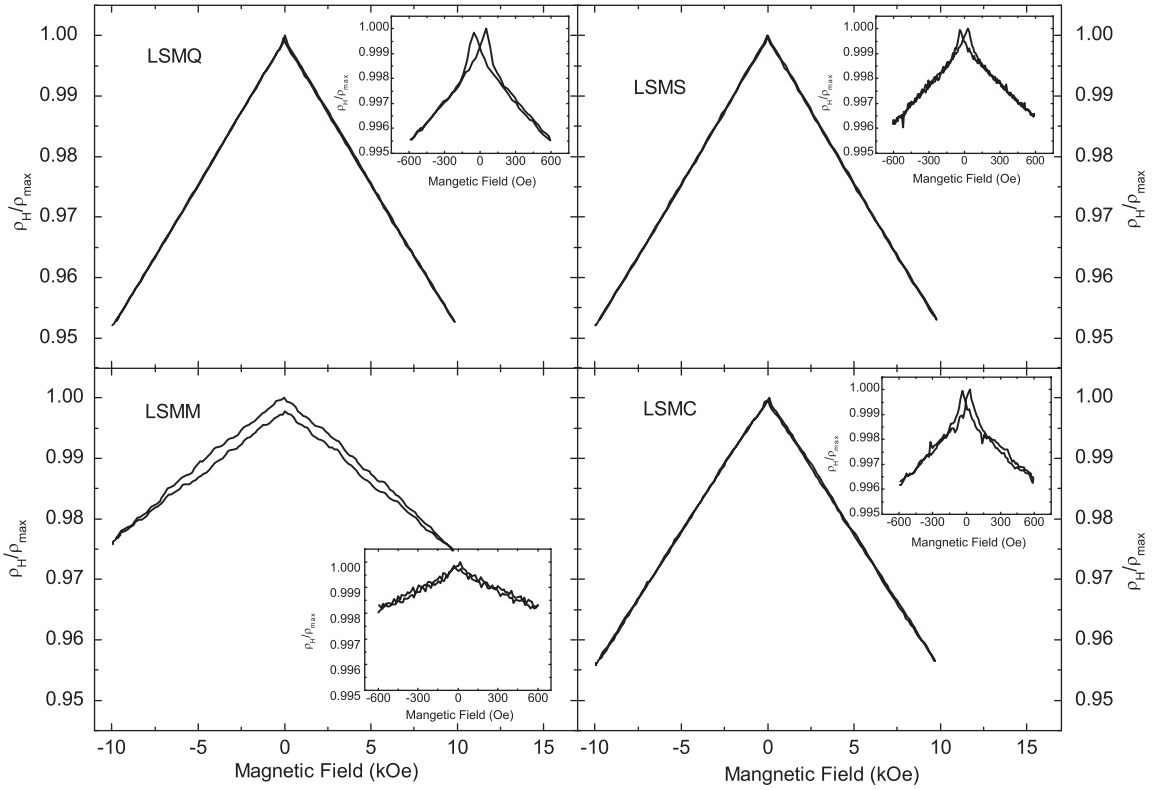

Fig. 5. Resistivity normalized to its maximum for all the LSMO films at 297 K (RT) as a function of applied field which is changed from +10 kOe to −10 kOe and back.

is the maximum resistivity that would not appear at zero field but near the coercive field of the film due to the hysteresis effect of resistivity as mentioned below. For all samples, the enlarged normalized resistivity-field dependence curves below 600 Oe are simultaneously embedded in Fig. 5. Low-field MR (LFMR) behavior and hysteresis of resistivity is observed in the embedded curves. The mechanism of the LFMR effect has been theoretically explained by Hwang et al. in detail [21]. Polycrystalline structure plays key role in the low-field MR effect, which would be dominated by the spin-polarized tunneling between grains. For our samples, the other kind of structural defects of porosity would devote to the LFMR effect. Furthermore, only when the polycrystalline CMR materials keep ferromagnetism below T_c, LFMR would occur. On the one hand, our samples present LFMR effect at RT. On the other hand, the hysteresis of resistivity reflects the close correlation between magnetotransport and magnetization. Near the coercive field the maximum resistivity would appear. So the occurrence of LFMR effect at RT for LSMQ and LSMM sample meets the fact that their T_C is beyond RT, and then it could be inferred that the LSMS and LSMC samples also present ferromagnetism and their T_C is also above RT, just like LSMQ and LSMM samples. Especially, for LSMM sample, the LFMR effect at RT is relatively weaker than the other samples. For LSMQ, LSMS and LSMC samples, their LFMR effect is similar and they present more pretty linear change of resistivity or MR with applied field scanning between −10 kOe to 10 kOe. The MR ratio of these samples under 10 kOe field reaches about 5%, twice that of the LSMM sample. These magnetotransport characteristics further demonstrate the more intensive substrate effect of LSMM sample than that of other three samples.

It is worth pointing out that, for all the samples except LSMM, their magnetotransport properties including similar resistivity-field dependences, pretty linearity of MR and considerable MR ratio at RT, should be significant to the application for LSMO films synthesized by low cost technique under the uses of simple MOD routine and the cheap substrates including amorphous quartz, silicon wafer and ceramic plates.

4. Conclusion

In summary, LSMO thin films were synthesized by means of MOD on different substrates. The XRD spectra show that all the samples are polycrystalline with (2 0 2) preferred orientation. The porous structural characteristics of the samples play key roles in the mechanism of magnetotransport of the samples, leading to the enhanced MR behavior below metal–insulator transition peak temperature (T_p) and LFMR effect. For LSMM samples, the facts of broad ferromagnetic–paramagnetic transition zone, lower T_p and weaker LFMR at RT reveal more intensive substrate effect of LSMO film synthesized on

(1 0 0) MgO single crystal. Furthermore, at RT the resistivity of all the samples except LSMM presents pretty linear change under applied field range and MR ratio gets to near 5% under 10 kOe field. The above magnetotransport properties show that MOD provides a low cost method for preparing applicable LSMO films on cheap substrates including amorphous quartz, silicon wafer and ceramic plates.

Acknowledgment

The authors would like to acknowledge the financial support from the State Key Laboratory of Functional Materials for Informatics, Shanghai Institute of Microsystem and Information Technology, Chinese Academy of Sciences.

References

[1] C. Moreno, C. Munuera, S. Valencia, F. Kronast, X. Obradors, C. Ocal, Reversible resistive switching and multilevel recording in $La_{0.7}Sr_{0.3}MnO_3$ thin films for low cost nonvolatile memories, Nano Letters 10 (2010) 3828–3835.

[2] D. Bahadur, D. Das, Properties of CMR composites, Proceedings of the Indian Academy of Sciences (Chemical Science) 115 (5–6) (2003) 587–606.

[3] L.W. Martin, Y.-H. Chu, R. Ramesh, Advances in the growth and characterization of magnetic, ferroelectric, and multiferroic oxide thin films, Materials Science and Engineering: R 68 (2010) 89–133.

[4] A. Rostamnejadi, M. Venkatesan, P. Kameli, H. Salamati, J.M.D. Coey, Magnetocaloric effect in $La_{0.67}Sr_{0.33}MnO_3$ manganite above room temperature, Journal of Magnetism and Magnetic Materials 323 (2011) 2214–2218.

[5] T. Tsuchiya, T. Nakajima, K. Daoudi, T. Kumagai, Electrical properties of the epitaxial $La_{1-x-y}Sr_xMnO_3$ films grown by excimer laser-assisted metal organic deposition, Materials Science and Engineering B 144 (2007) 89–92.

[6] M. Shiraishi, T. Ikoma, Molecular spintronics, Physica E 43 (2011) 1295–1317.

[7] M.C. Terzzoli, D. Rubi, S. Duhalde, M. Villafuerte, M. Sirena, L. Steren, Transport properties of pulsed laser deposited $La_{0.67}Sr_{0.33}MnO_3$ thin films, Applied Surface Science 186 (2002) 458–462.

[8] J. Coulon, A. Hassini, M. Gervais, F. Gervais, C. Champeauxc, A. Catherinot, Growing and characterization of $La_{0.8}Sr_{0.2}MnO_3$ thin films on single crystal oxide substrate, Materials Science and Engineering B 104 (2003) 141–144.

[9] J.Y. Gu, S.B. Ogale, M. Rajeswari, T. Venkatesan, R. Ramesh, V. Radmilovic, U. Dahmen, G.. Thomas, T.W. Noh, In-plane grain boundary effects on the magnetotransport properties of $La_{0.7}Sr_{0.3}MnO_{3-\delta}$, Applied Physics Letters 72 (1998) 1113–1115.

[10] S.P. Isaac, N.D. Mathur, J.E. Evetts, M.G. Blamire, Magnetoresistance of artificial $La_{0.7}Sr_{0.3}MnO_3$ grain boundaries as a function of misorientation angle, Applied Physics Letters 72 (1998) 2038–2040.

[11] G.L. Yuan, J.-M. Liu, H.L.W. Chan, C.L. Choy, C.K. Ong, Z.G. Liu, Y.W. Du, Low-field magnetoresistance in oxygen-deficient $La_{0.5}Sr_{0.5}MnO_3$ thin films as approached by spin-polarized tunneling model, Materials Letters 53 (2002) 76–82.

[12] D. Liu, W. Liu, Growth and characterization of epitaxial $(La_{2/3}Sr_{1/3})MnO_3$ films by pulsed laser deposition, Ceramics International 37 (2011) 3531–3534.

[13] D.R. Sahu, The properties of $La_{0.7}Sr_{0.3}MnO_3$ films prepared by dc magnetron sputtering using nanosized powder compacted target: effect of substrate temperature, Applied Surface Science 255 (2008) 1870–1873.

[14] Z. Yang, L. Sun, C. Ke, X. Chen, W. Zhu, O. Tan, Growth and structure properties of $La_{1-x}Sr_xMnO_{3-\sigma}$ ($x=0.2$, 0.3, 0.45) thin film grown on $SrTiO_3$ (0 0 1) single-crystal substrate by laser molecular beam epitaxy, Journal of Crystal Growth 311 (2009) 3289–3294.

[15] L. Meda, K.H. Dahmen, S. Hayek, H. Garmestani, X-ray diffraction residual stress calculation on textured $La_{2/3}Sr_{1/3}MnO_3$ thin film, Journal of Crystal Growth 263 (2004) 185–191.

[16] M. Nasui, T. Petrisor Jr., R.B. Mos, M.S. Gabor, T. Ristoiu, A. Rufoloni, L. Ciontea, T. Petrisor, Precursor chemistry for the solution deposition of epitaxial $La_{0.66}Sr_{0.33}MnO_3$ (LSMO) thin films, Thin Solid Films 518 (2010) 4753–4756.

[17] X.R. Zhu, H.L. Shen, Z.X. Tang, K. Tsukamoto, T. Yanagisawa, M. Okutomi, N. Higuchi, Structural and magnetotransport properties of $La_{0.67}Sr_{0.33}MnO_z$ thin films prepared by metal–organic decomposition under different annealing process, Journal of Alloys and Compounds 488 (2009) 437–441.

[18] M. Španková, Š. Chromik, I. Vávra, K. Sedláčková, P. Lobotka, S. Lucas, S. Stanček, Epitaxial LSMO films grown on MgO single crystalline substrates, Applied Surface Science 253 (2007) 7599–7603.

[19] T. Manabe, T. Fujimoto, I. Yamaguchi, W. Kondo, I. Kojima, S. Mizuta, T. Kumagai, Effects of substrate materials and annealing temperature on crystal structure and epitaxy of $La_{0.7}Sr_{0.3}MnO_3$ films via dipping–pyrolysis process, Thin Solid Films 323 (1998) 99–104.

[20] A. Urushibara, Y. Moritomo, T. Arimo, A. Asamitsu, G. Kido, Y. Tokura, Insulator-metal transition and giant magnetoresistance in $La_{1-x}Sr_xMnO_3$, Physical Review B 51 (1995) 14103–14109.

[21] H.Y. Hwang, S-W. Cheong, N.P. Ong, B. Batlogg, Physical Review Letters 77 (1996) 2041–2044.

[22] A.J. Millis, T. Darling, A. Migliori, Quantifying strain dependence in colossal magnetoresistance manganites, Journal of Applied Physics 83 (1998) 1588–1591.

[23] C. Adamo, X. Ke, Q. Wang, L. Xin, T. Heeg, M.E. Hawley, W. Zander, J. Schubert, P. Schiffer, D.A. Muller, L. Maritato, D.G. Schlom, Effect of biaxial strain on the electrical and magnetic properties of (001) $La_{0.7}Sr_{0.3}MnO_3$ thin films, Applied Physics Letters 95 (2009) 112504.

[24] S. Majumdar, H. Huhtinen, H.S. Majumdar, P. Paturi, Stress and defect induced enhanced low field magnetoresistance and dielectric constant in $La_{0.7}Sr_{0.3}MnO_3$ thin films, Journal of Alloys and Compounds 512 (2012) 332–339.

[25] X.L. Wang, S.X. Dou, H.K. Liu, M. Ionescu, B. Zeimetz, Large low-field magnetoresistance over a wide temperature range induced by weak-link grain boundaries in $La_{0.7}Ca_{0.3}MnO_3$, Applied Physics Letters 73 (1998) 396–398.